Thickness of the air-water interface from first-principles simulation-based hydrogen bond dynamics

Gang Huang[1, a)] and Jie Huang[2, b)]
[1)] *Institute of Theoretical Physics, Chinese Academy of Sciences, Zhongguancun East Road 55, 100190 Beijing, China*
[2)] *Department of Physics, Wenzhou University, 325006 Wenzhou, China*

(Dated: 23 April 2022)

The thickness of the air-water interface is determined by interface hydrogen bond (HB) dynamics. By density functional theory-based molecular dynamics (DFTMD) simulations, two extreme cases of the interface HB dynamics are obtained: one underestimates the HB breaking rate constant and the other overestimates it. The interface HB dynamics in these two cases tends to be the same as the thickness of the air-water interface increases to 4 Å. The interface thickness is determined when the interface HB dynamics under the two cases is converged.

I. INTRODUCTION

The air-water interface has been a subject of extensive studies due to its ubiquity in nature and its importance as a model system for aqueous hydrophobic interfaces[1]. It is widely accepted that water molecules behave differently at the interface than in bulk phase[2]. Estimating the thickness of the air-water interface is a debated subject, and has been studied over the past years[3].

The air-water interface thickness has experimentally been measured via both ellipsometry[4–6] and X-ray reflectivity[7]. There are some general consensus on the fact that the thickness is about 3–10 Å[8]. Nonetheless, accurately determining the thickness of the air-water interface remains experimentally challenging.

In recent years, computer simulation techniques have been used to determine the air-water interface thickness[9–11]. In previous computer simulations, the defined thickness of the interface depends on the parameters chosen manually, such as the 10%–90% thickness[12–19] and Levenberg-Marquardt least-square fit[20]. In addition, the density-based definition of interface thickness faces a debate over the reality of the oscillations of the density profile[21]. Besides, interface thickness is a sensitive quantity to the intermolecular potential and treatment of long-range correction[14,15], and the accuracy of MD simulations are limited by the accuracy of the potential functions being used[13]. Density functional theory-based molecular dynamics (DFTMD) simulations[9,10,22] offer a predictive platform for density profiles and the thickness of the air-liquid interfaces[23]. Using DFTMD simulations Sulpizi *et al.*[10] (Pezzotti, Galimberti, and Gaigeot[11]) have calculated the second-order nonlinear susceptibility for the pre-defined instantanously interfacial layers[24] and deduced a thickness of 3 Å (3.5 Å) of air-water interface at 330 K (315 K). Therefore, the existing simulation methods for determining the air-water interface thickness mainly fall into two categories: (1) Using classical molecular dynamics simulations and artificially selected parameters to determine the thickness of the interface; (2) Using first-principles molecular dynamics simulations and interfacial layer difference in properties to infer the thickness of the interface.

Therefore, a more natural method for estimating the air-water interface thickness, which has the following features are needed: (1) It does not depend on the interaction potential functions. (2) It does not depend on the choice of parameters, or it avoid the direct definition of interface thickness in terms of density. In this paper, DFTMD simulations are used to satisfy (1), and a combination of interfacial molecule sampling (IMS) and a newly defined interface HB (IHB) population methods was used to satisfy (2).

We determine the thickness of air-water interface from the perspective of hydrogen bond (HB) dynamics of instantaneous interface. Our approach naturally distinguishes the boundary between interface and bulk water, which depends on the convergence of properties of the interface hydrogen (H-) bonds. The two methods, IMS and IHB, give the HB dynamics of the air-water interface from two extreme cases. The combination of the them has a surface selectivity, and a more realistic HB dynamics of the air-water interface and thus the interface thickness is obtained. The calculated thickness of the air-water interface at room temperature is about 4 Å.

The paper is organized as follows. In Sec. II we review the HB population operator and related correlation functions, and the method to obtain the HB breaking and reforming rate constants. Section III then introduces the ideas of IHB and IMS to identify interface H-bonds. The main results and discussions are presented in Sec. IV. Finally, the conclusions are presented in Sec. V.

II. HYDROGEN BOND DYNAMICS

Using a geometric criterion of HB, Luzar and Chandler[25] have pioneered the analysis of HB dynamics of pure water, and subsequently such analysis has been extended to more complex systems, e.g., electrolytes[26], protein[27] and micellar surfaces[28]. In the criterion, two water molecules are H-bonded if their interoxygen distance r_{OO} is less than cutoff radius[29] $r_{OO}^{c} = 3.5$ Å and the H-O$\cdots$O angle ϕ (see Fig 1) is less than cutoff angle[30–33] $\phi^{c} = \pi/6$. We denote it as acceptor-donor-hydrogen (ADH) criterion. For comparison,

[a)] Electronic mail: hg08@lzu.edu.cn
[b)] Electronic mail: jiehuang@stu.wzu.edu.cn

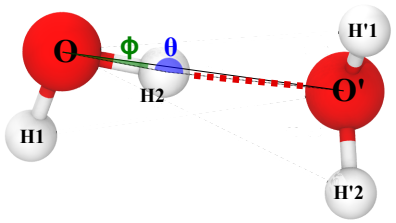

FIG. 1. Two HB criteria depending on OO′ distance and angles θ or ϕ.

we also use another HB criterion: r_{OO} is less than r^c_{OO}, and the O-H$\cdots$O included angle θ is greater than cutoff angle[1] $\theta^c = 2\pi/3$. We denote this HB criterion as the acceptor-hydrogen-donor (AHD) criterion.

We use a configuration $r(t)$ denotes the positions of all the atoms in the system at time t. Either of the criteria above allows one to define a HB population $h[r(t)] = h(t)$, which equals 1 when a tagged pair of molecules are H-bonded, and 0 otherwise. The fluctuation in $h(t)$ from its time-independent equilibrium average is defined by[34] $\delta h = h(t) - \langle h \rangle$. The probability that a specific pair of molecules is H-bonded in a large system is extremely small, then $\delta h(t) = h(t)$. Therefore, the correlation of $\delta h(t)$ can be written as

$$\langle \delta h(0)\delta h(t)\rangle = \langle h(0)h(t)\rangle,$$

where the averaging $\langle\cdots\rangle$ is to be performed over the ensemble of initial conditions.

A. Hydrogen bond correlation functions

The correlation function[26,35]

$$c(t) = \langle h(0)h(t)\rangle / \langle h\rangle \tag{1}$$

describes the structural relaxation of H-bonds. Here the average $\langle h\rangle$ of the HB population is the probability that a pair of randomly chosen water molecules in the system is H-bonded at any time t. The function $c(t)$ measures correlation in $h(t)$ independent of any possible bond breaking events, and it relaxes to zero, when t is large[36].

Because the thermal motion can cause distortions of H-bonds from the perfectly tetrahedral configuration, water molecules show a librational motion on a time scale of ~ 0.1 ps superimposed to rotational and diffusional motions (> 1 ps), which causes a time variation of interaction parameters. A new HB population $h^{(d)}(t)$ was also defined to obviate the distortion of real HB dynamics due to the above geometric definition[26,29]. It is 1 when the interoxygen distance of a particular tagged pair of water molecules is less than r^c_{OO} at time t, and 0 otherwise. The H-bonds between a tagged molecular pair that satisfy the condition $h^{(d)}(t) = 1$ may have been broken, but they may more easily form H-bonds again. The correlation function

$$n(t) = \langle h(0)[1-h(t)]h^{(d)}(t)\rangle / \langle h\rangle \tag{2}$$

represents the probability at time t that a tagged pair of initially H-bonded water molecules are unbonded but remain separated by less than r^c_{OO}[26].

The rate of HB relaxation to equilibrium is characterized by the reactive flux[37]

$$k(t) = -\frac{dc(t)}{dt}, \tag{3}$$

which quantifies the rate that an initially present HB breaks at time t, independent of possible breaking and reforming events in the interval from 0 to t. Therefore, $k(t)$ measures the effective decay rate of an initial set of H-bonds[34]. For bulk water, there exists a ~ 0.2-ps transient period, during which $k(t)$ changes quickly from its initial value[38]. However, at longer times, $k(t)$ is independent of the HB definitions.

B. Hydrogen bond breaking and reforming rate constants

Assume that each HB acts independently of other H-bonds[25,37], and due to detailed balance condition, one obtain $\tau_{HB} = (1-\langle h\rangle)/k$, where k is the rate constant of breaking a HB, i.e., the forward rate constant[39,40]. Correspondingly, the backward rate constant k' is represented by the rate constant from the HB *on* state to the HB *off* state for a tagged pair of molecules. Based on the functions $n(t)$, $h(t)$, $h^{(d)}(t)$, and $k(t)$, Khaliullin and Kühne[22] have obtained the ratio k/k' of HB breaking and reforming rate constants in bulk water, and then the lifetime and relaxation time of H-bonds from simulations. Here, for the air-water interface, we obtain the optimal solution range of k and k' from the relationship between the reactive flux $k(t)$ and the correlation functions $c(t)$ and $n(t)$:

$$k(t) = kc(t) - k'n(t). \tag{4}$$

We obtain the optimal value of the rate constants, k and k', by a least squares fit of $k(t)$, $c(t)$ and $n(t)$ beyond the transition phase. The function $c(t)$ is regarded as a column vector composed by $(c_1,\cdots,c_P)^{\mathsf{T}}$, and is denoted as $\mathbf{c}$, with c_i representing the value of correlation $c(t)$ at $t = i$. Similarly, $n(t)$ and $k(t)$ can also be denoted as $\mathbf{n}$ and $\mathbf{k}$, respectively. Then, the rate constants k and k' are determined from the matrix $\mathbf{A} = [\mathbf{c}\ \ \mathbf{n}]$:

$$\begin{bmatrix} k \\ -k' \end{bmatrix} = (\mathbf{A}^{\mathsf{T}}\mathbf{A})^{-1}\mathbf{A}^{\mathsf{T}}\mathbf{k}. \tag{5}$$

For bulk water and the air-water interface, the optimal k and k' are reported in Table I and II.

TABLE I. The rate constants k and k' for the bulk water and the air-water interface (the time region 0.2 ps $< t <$ 2 ps).

Criterion	k (b)[a]	k' (b)	τ_{HB} (b)[b]	k (i)	k' (i)	τ_{HB} (i)
ADH	0.296	0.988	3.380	0.323	0.765	3.101
AHD	0.288	1.149	3.470	0.314	0.887	3.184

[a] The unit for k (k') is ps^{-1}. b: bulk; i: interface.
[b] The unit for τ_{HB} ($= 1/k$) is ps.

TABLE II. The k and k' for the bulk water and the air-water interface (the time region 2 ps $< t <$ 12 ps).

Criterion	k (b)	k' (b)	τ_{HB} (b)	k (i)	k' (i)	τ_{HB} (i)
ADH	0.115	0.039	8.718	0.157	0.068	6.372
AHD	0.105	0.047	9.496	0.155	0.088	6.472

To obtain k and k', we performed the fitting in short and long time regions, respectively. We note that in the long time region ($2 < t < 12$ ps), the value of HB lifetime τ_{HB} is larger than that in short one ($0.2 < t < 2$ ps), no matter for the bulk water or for the air-water interface. A larger τ_{HB} value means that the distance between a pair of water molecules stays within r^c_{OO} for a longer time.

C. Computational Methods

To describe the subtleties of H-bonding in water[41], we have performed DFTMD simulations[42] for bulk water and the air-water interface. The simulations make use of some technologies that have been successfully tested on water and solutions[10,43–45], namely the Goedecker-Teter-Hutter (GTH) pseudopotentials[46–48], Generalised Gradient Approximation (GGA) of the exchange-correlation functional[49,50], and dispersion force correction, DFT-D3[51,52]. By eliminating the strongly bound core electrons, the GTH pseudopotentials reduce the number of occupied electronic orbitals that have to be treated in an electronic structure calculation. There are dual-space Gaussian-type pseudopotentials that are separable and satisfy a quadratic scaling with respect to system size[53]. The GGA functionals generally describe the dipole and quadruple moments of the molecules quite well; and DFT-D3 correction can treat the van der Waals dispersion forces in DFT and improve the structural properties without more computational cost, and thus can be used at the air-water interface.

The DFTMD calculation is implemented by a NVT code that implemented in the CP2K/QUICKSTEP package[54,55]. The BLYP XC functional, which consists of Becke non-local exchange[49] and Lee-Yang-Parr correlation[50] have been employed. The electron-ion interactions are described by GTH pseudopotentials[47,56]. A Gaussian basis for the wave functions and an auxiliary plane wave bisis set for the density are used in this scheme. DZVP-GTH basis set is used for all atoms and a cutoff of 280 Ry is chosen for the charge density[54]. The Nosé-Hoover chain thermostat[57] is used to conserve the temperature at 300 K. The simulation for the air-water interface use a time step of 0.5 fs.

The bulk water system consisted of 128 water molecules in a periodic box of size $15.64 \times 15.64 \times 15.64$ Å^3, and with a density of 1.00 g cm^{-3}. The slab consisted of 128 water molecules in a periodic box of size $15.64 \times 15.64 \times 31.28$ Å^3. The length of each trajectory in each simulation is $t_{traj} = 60$ ps. The RDFs $g_{OO}(r)$ and $g_{OH}(r)$ for the bulk water systems are shown in Fig. 2. The probability distribution of O and H atoms in the simulated model of air-water interface is showed in Fig. 3.

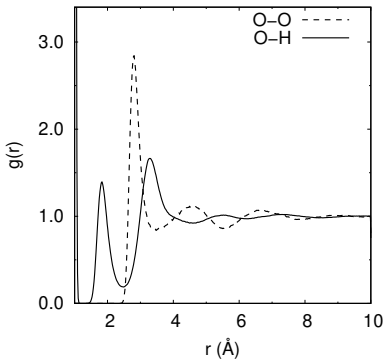

FIG. 2. The partial radial distribution functions (RDFs) for the simulated bulk water system.

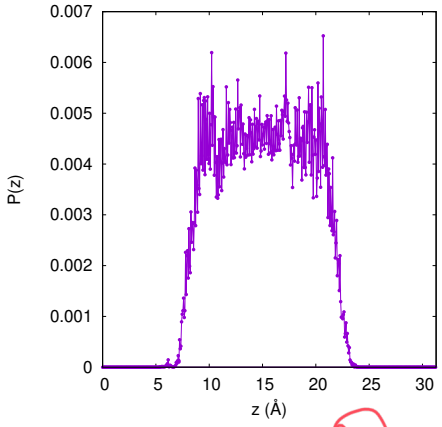

FIG. 3. Probability distribution $P(z)$, along z-axis, of H_2O in the slab.

III. HB DYNAMICS FOR INSTANTANEOUS AIR-WATER INTERFACE

Due to molecular motions, the identity of molecules that lie at the interface changes with time, and generally useful procedures for identifying interface must accommodate these motions. To determine the instantaneous air-water interface, we here adopt a spatial density-based method proposed by Willard and Chandler[24]. and then the air-water boundary is modeled with the Willard-Chandler instantaneous surface[24,58]. Figure 4 illustrates the obtained interfaces for one configuration of a slab of pure water.

For the slab in the cuboid simulation box, we can get another surface $\mathbf{s}_0(t)$ by translating the surface $\mathbf{s}(t)$ along the system's normal (into bulk) to a distance d. The region between the two surfaces $\mathbf{s}(t)$ and $\mathbf{s}_0(t)$ is defined as *the air-water interface*. We have obtained HB dynamics at the instantaneous air-water interface, and there are two extreme cases to be considered.

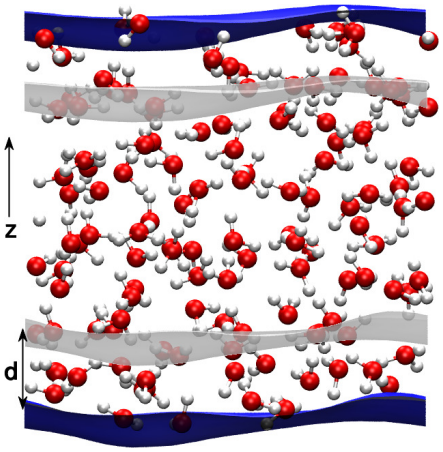

FIG. 4. A slab of water with the instantaneous surface **s** represented as a blue mesh on the upper and lower phase boundary. The normal is along the z-axis and d is the thickness of the interface. The grey surface is obtained by translating the surface to the inside of the system along the z-axis by d.

A. Hydrogen bond dynamics based on interfacial molecule sampling

As the first method to obtain interface HB dynamics, we use molecule sampling at the instantaneous interface. Let T_e be the time it takes for all water molecules in the simulation box to traverse the interface and bulk phase. If the trajectory length $t_{\rm traj}$ satisfies the condition $\tau_{\rm HB} \ll t_{\rm traj} \ll T_e$, one find M time points t_i, $(i = 1, \cdots, M)$ that are evenly spaced on the trajectory, then one obtain interface HB dynamics using the following procedure:

1. For each observation time t_i, define an interface with a thickness d (see Fig. 4). Then, select a set S_i of water molecules which are at the interface, and calculate the correlation functions $c_i(t)$, $n_i(t)$ and $k_i(t)$ through $t_{\rm traj}$ for the molecules that belong to the set S_i.

2. Determine average functions $c(t)$, $n(t)$ and $k(t)$, of the correlation functions $c_i(t)$, $n_i(t)$ and $k_i(t)$ over M sampling time points respectively.

3. Determine reaction rate constant of breaking and reforming at the interface with thickness d, by Eq.4.

In the IMS method, since the configuration of molecules changes over time, the contribution of H-bonds in bulk phase is included. Therefore, the IMS method *understimates* the HB breaking rate constant of the interface.

B. Hydrogen bond dynamics based on interface HB population

After determining the instantaneous interface, we introduce an interface HB population operator $h^{(s)}[\mathbf{r}(t)]$ as follows: It has a value 1 when a tagged molecular pair i, j are H-bonded *and* both molecules are at the interface with a thickness d, and 0 otherwise:

$$h^{(s)}[\mathbf{r}(t)] = \begin{cases} 1 & i,j \text{ are H-bonded, } \textit{and} \\ & i,j \text{ are at the interface;} \\ 0 & \text{otherwise.} \end{cases} \quad (6)$$

Then the correlation function $c^{(s)}(t)$ that describes the fluctuation of H-bonds *at the interface*:

$$c^{(s)}(t) = \langle h^{(s)}(0) h^{(s)}(t) \rangle / \langle h^{(s)} \rangle, \quad (7)$$

can be obtained.

Similar to Eq. 2 and Eq. 3, the corresponding correlation function

$$n^{(s)}(t) = \langle h^{(s)}(0)[1 - h^{(s)}(t)] h^{(d,s)} \rangle / \langle h^{(s)} \rangle, \quad (8)$$

and interface reactive flux function

$$k^{(s)}(t) = -\frac{dc^{(s)}(t)}{dt} \quad (9)$$

are obtained. The $h^{(d,s)}(t)$ is 1 when the a tagged pair of water molecules i, j are *at the interface* and the interoxygen distance between the two molecules is less than $r_{\rm OO}^c$ at time t, and 0 otherwise, i.e.,

$$h^{(d,s)}[\mathbf{r}(t)] = \begin{cases} 1 & i,j \text{ are at the interface} \\ & \text{and } |\mathrm{O}_i\mathrm{O}_j| < r_{\rm OO}^c; \\ 0 & \text{otherwise.} \end{cases} \quad (10)$$

Therefore, $n^{(s)}(t)$ represents the prabability at time t that a tagged pair of initially H-bonded water molecules at the interface are unbonded but remain at the interface and separated by less than $r_{\rm OO}^c$; $k^{(s)}(t)$ measures the effective decay rate of H-bonds at the interface. The functions defined in Eq.7–9 are used to determine the reaction rate constant of breaking and reforming and the lifetimes of H-bonds at the interface by Eq.4, in which $c(t)$, $n(t)$ and $k(t)$ are replaced by $c^{(s)}(t)$, $n^{(s)}(t)$ and $k^{(s)}(t)$.

In the IHB method, it is accurate to choose the water molecules and H-bonds at the interface. However, for some special H-bonds, if it connects such two water molecules, one is at the interface and the other is in bulk water. Then the HB reaction rate of such H-bonds will be artificially increased. Therefore, unlike the IMS method, the IHB method *overestimates* the HB breaking rate constant.

IV. DISCUSSIONS: EFFECTS OF AIR-WATER INTERFACE ON HYDROGEN BOND DYNAMICS

A. Hydrogen bond relaxation

Two geometric criteria of H-bonds are used to calculate the $h^{(s)}(t)$, and the corresponding $c^{(s)}(t)$ from Eq.7 are shown in Fig. 5. We found that as d increases, $c^{(s)}(t)$ at the interface relaxes more slowly. When d is greater than 4 Å, $c^{(s)}(t)$ recovers the bulk value. This feature is independent of the HB definition as shown by the comparison of results in panel a and b of

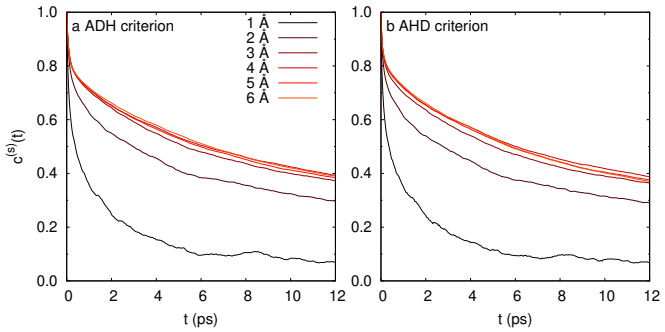

FIG. 5. The $c^{(s)}(t)$ for interface H-bonds with differnt thickness d, based on HB population operator $h^{(s)}(t)$, as computed from the (a) ADH and (b) AHD criteria of H-bonds.

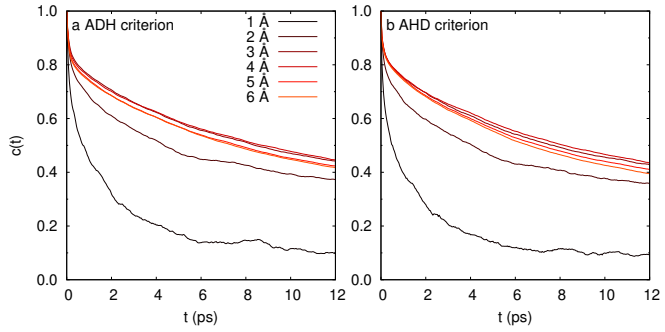

FIG. 6. The $c(t)$ for H-bonds at the interfaces with different d, based on HB population operator $h(t)$, as computed from the (a) ADH and (b) AHD criteria of H-bonds. These results are based on the IMS method, in which the sampling is performed every 4 ps.

Fig. 5. Figure 6 shows the d-dependence of $c(t)$. Comparing Fig.s 5 and 6, We find that $c(t)$ has the same feature: as d increases, $c(t)$ also relaxes more slowly; when d is greater than 4 Å, $c^{(s)}(t)$ also approaches a stable function. Comparing $c(t)$ and $c^{(s)}(t)$, the second feature is that for the same d, the value of $c(t)$ is always slightly larger than $c^{(s)}(t)$. Moreover, regardless of the AHD or ADH criterion of H-bonds, these two features are valid. The first feature is the general one of interface H-bonds, while the second feature is derived from the difference in the definitions of HB population operators $h(t)$ and $h^{(s)}(t)$. Using this difference between $h(t)$ and $h^{(s)}(t)$, we can obtain the HB dynamics of the real interface, especially the thickness of the interface.

B. Hydrogen bond breaking and reforming rate constants

To find the reaction rate constants k and k', we start from the correlation functions $c^{(s)}(t)$, $n^{(s)}(t)$ and $k^{(s)}(t)$, (or $c(t)$, $n(t)$ and $k(t)$) of the H-bonds that are at the interface at time t. Figure 7 compares the rate constants and the lifetime τ_{HB} obtained by the IHB and interface molecule selection (IMS) methods. We find that, for all the three quantities k, k' and τ_{HB}, the behavior as function of the thickness of the interface is hardly affected by the calculation methods. To illustrate this point more clearly, we compare the k, k' and τ_{HB} obtained under the two methods.

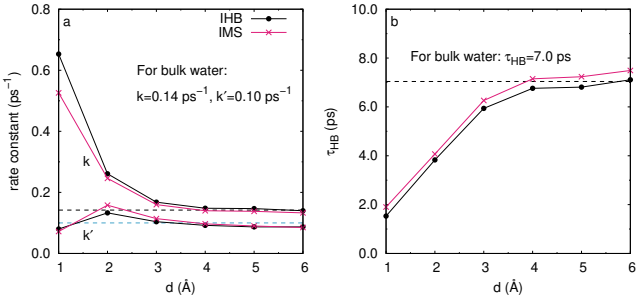

FIG. 7. The dependence of (a) the rate constants k and k' and (b) the HB lifetime τ_{HB} on the interface thickness, obtained by the IHB and the IMS method, respectively. The corresponding k, k' and τ_{HB} in bulk water are also drawn with dashed lines as a reference. In sub-figure (a), the k of bulk water is represented by a black dashed line, and the k' by a blue dashed line; in sub-figure (b), the τ_{HB} of bulk water is represented by a black dashed line. The ADH criterion is used and the fits are carried on the time region 0.2 ps $< t <$ 12 ps.

From Fig. 7, one can find that the constants k and k' obtained by the two methods agree quantitatively, when d is larger than d_0 =4 Å.

The forward rate constant k obtained by using the IHB method is relatively larger than that from the IMS method, and backward rate constant k' is relatively smaller. Since $\tau_{HB} \approx 1/k$, this directly leads to a relatively shorter HB lifetime using the IHB method. This result is related to the definitions of $h(t)$ and $h^{(s)}(t)$. The definition of $h^{(s)}(t)$ makes the HB break rate at the interface artificially increased. The IMS method, which is based on $h(t)$, retains the original rate constant of H-bonds, but it may include the contribution of bulk water molecules to the rate constant.

In Fig. 7, the k, k' and τ_{HB} for the *bulk* water are also drawn with dashed lines as a reference. Comparing the above-mentioned physical quantities at the air-water interface and bulk water, we find that when the interface thickness is larger than 4 Å, no matter which statistical method is used, the obtained reaction rate constants of the interface water is *greater* than that in bulk water. Therefore, the HB lifetime $\tau_{HB} = 1/k$ in interface water is smaller than that in bulk water.

Furthermore, we find from Fig. 7 that as d increases, k and k' gradually close to the rates in bulk water at the same condition. These results are obtained by the least squares method in the same interval (0.2–12 ps). They show that the IHB method can get results as good as the IMS method when d is larger than 4 Å.

The above two methods respectively give an extreme case of interface HB dynamics. In other words, the calculated HB dynamics obtained by IHB method is *accelerated*, compared to the real one. Real HB dynamics of the interface is between the results of the above two methods. Naturally, we approximate the true HB dynamics of the interface, by combining both the IHB and IMS methods. In these two extreme cases the interface HB characteriestics tends to be the same as the

thickness of the interface increases. Properties such as the HB lifetime, HB reaction rate constants, and the thickness of the air-water interface can be estimated. For example, as the parameter d increases, when all the k, k', τ_{HB} of the interface calculated by both methods become consistent, the value of d is the thickness of the air-water interface.

V. CONCLUSIONS

Based on the DFTMD simulations, the IMS method partially gives information on the HB breaking and reforming reaction rate constants through the air-water interface and therefore partially shows how much the interface affects dynamics of H-bonds in water. The IHB method also provides partial information on the HB breaking and reforming reaction rates at the interface. As the thickness of interface increases, comparing results in the two extreme cases, we find that the HB breaking and reforming rate constants at the air-water interface tends to be uniform. Therefore, the real HB dynamical characteristics at the air-water interface can be derived. We conclude that from the perspective of HB dynamics, the thickness of the air-water interface at room temperature is 4 Å. In other words, at this thickness the HB dynamical properties of air-water interface become the same as bulk water.

The idea of combinating IHB and IMS can naturally be extended to the solution interface. This method of determining interface thickness can be extended to other interfacial systems, so that the boundary between interface and bulk phase can be naturally determined. For the systems where statistical properties of the interface and bulk phase differ significantly, these differences will be represented more appropriately. In addition, the IHB method itself can also be extended. For example, one can combine the HB population with the hydration shell of ions.

Appendix: The published values of the air-water interface thickness

TABLE III. The air-water interface thickness obtained by experiments.

Method	T	d (Å)
Ellipsometry (Rayleigh)	20°C	3.0
Ellipsometry (Raman and Ramdas [4])	20°C	5.0
Ellipsometry (McBain, Bacon, and Bruce [5])	20°C	≥2.26
Ellipsometry (Kinosita and Yokota [6])	20°C	7.1
X-Ray Reflectivity(Braslau *et al.* [59])	25 °C	3.24± 0.05
-	-	roughness/thickness?

ACKNOWLEDGMENTS

GH acknowledges the financial support of the China Scholarship Council. The simulations were performed on the Mogon ZDV cluster in Mainz and on the Cray XE6 (Hermit) at the HRLS supercomputing center in Stuttgart.

[1] J. Jeon, C.-S. Hsieh, Y. Nagata, M. Bonn, and M. Cho, "Hydrogen bonding and vibrational energy relaxation of interfacial water: A full dft molecular dynamics simulation," J. Chem. Phys. **147**, 044707 (2017), https://doi.org/10.1063/1.4995437.
[2] L. X. Dang and T.-M. Chang, "Molecular dynamics study of water clusters, liquid, and liquid-vapour interface of water with many-body potentials," J. Chem. Phys. **106**, 8149 (1997).
[3] P. K. Nandi, N. J. English, Z. Futera, and A. Benedetto, "Hydrogen-Bond Dynamics at the Bio-Water Interface in Hydrated Proteins: A Molecular-Dynamics Study," Phys. Chem. Chem. Phys. **19**, 318–329 (2017).
[4] C. Raman and L. Ramdas, "On the thickness of the optical transition layer in liquid surfaces," Phil. Mag. **3**, 220 (1927).
[5] J. W. McBain, R. C. Bacon, and H. D. Bruce, "Optical surface thickness of pure water," The Journal of Chemical Physics **7**, 818–823 (1939), https://doi.org/10.1063/1.1750531.
[6] K. Kinosita and H. Yokota, "Temperature dependence of the optical surface thickness of water," J. Phys. Soc. Japan **20**, 1086 (1965).
[7] A. Braslau, M. Deutsch, P. S. Pershan, A. H. Weiss, J. Als-Nielsen, and J. Bohr, "Surface roughness of water measured by x-ray reflectivity," Phys. Rev. Lett. **54**, 114–117 (1985).
[8] Y. Peng, Z. Tong, Y. Yang, and C. Q. Sun, "The Common and Intrinsic Skin Electric-Double-Layer (EDL) and Its Bonding Characteristics of Nanostructures," Applied Surface Science **539**, 148208 (2021).
[9] T. D. Kühne, T. A. Pascal, E. Kaxiras, and Y. Jung, "New Insights into the Structure of the Vapor/Water Interface from Large-Scale First-Principles Simulations," J. Phys. Chem. Lett. **2**, 105–113 (2011).
[10] M. Sulpizi, M. Salanne, M. Sprik, and M.-P. Gaigeot, "Vibrational sum frequency generation spectroscopy of the water liquid-vapor interface from density functional theory-based molecular dynamics simulations," J. Phys. Chem. Lett. **4**, 83–87 (2013), http://dx.doi.org/10.1021/jz301858g.
[11] S. Pezzotti, D. R. Galimberti, and M.-P. Gaigeot, "2D H-Bond Network as the Topmost Skin to the Air-Water Interface," J. Phys. Chem. Lett. **8**, 3133–3141 (2017).
[12] D. Beaglehole and P. Wilson, "Thickness and Anisotropy of the Ice-Water Interface," J. Phys. Chem. **97**, 11053–11055 (1993).
[13] R. S. Taylor, L. X. Dang, and B. C. Garrett, "Molecular Dynamics Simulations of the Liquid/Vapor Interface of SPC/E Water," J. Phys. Chem. **100**, 11720–11725 (1996).
[14] V. P. SOKHAN and D. J. TILDESLEY, "The free surface of water: molecular orientation, surface potential and nonlinear susceptibility," Molecular Physics **92**, 625–640 (1997), https://doi.org/10.1080/002689797169916.
[15] A. Morita and J. T. Hynes, "A theoretical analysis of the sum frequency generation spectrum of the water surface," Chem. Phys. **258**, 371–390 (2000).
[16] S. Paul and A. Chandra, "Dynamics of water molecules at liquid-vapour interfaces of aqueous ionic solutions: effects of ion concentration," Chemical Physics Letters **373**, 87–93 (2003).
[17] S. Paul and A. Chandra, "Hydrogen bond dynamics at vapour-water and metal-water interfaces," Chemical Physics Letters **386**, 218–224 (2004).
[18] A. Morita, "Improved computation of sum frequency generation spectrum of the surface of water," J. Phys. Chem. B **110**, 3158–3163 (2006).
[19] J. Zhao, G. Yao, S. B. Ramisetti, R. B. Hammond, and D. Wen, "Molecular dynamics simulation of the salinity effect on the n-decane/water/vapor interfacial equilibrium," Energy Fuels **32**, 11080–11092 (2018).
[20] M. Sega and C. Dellago, "Long-range dispersion effects on the water/vapor interface simulated using the most common models," J. Phys. Chem. B **121**, 3798–3803 (2017).
[21] R. Evans, J. Henderson, D. Hoyle, A. Parry, and Z. Sabeur, "Asymptotic decay of liquid structure: oscillatory liquid-vapour density profiles and the Fisher-Widom line," Molecular Phys. **80**, 755–775 (1993).
[22] R. Z. Khaliullin and T. D. Kühne, "Microscopic properties of liquid water from combined ab initio molecular dynamics and energy decomposition studies," Phys. Chem. Chem. Phys. **15**, 15746–15766 (2013).
[23] F. J. Blas, E. M. D. Río, E. D. Miguel, and G. Jackson, "An examination of the vapour-liquid interface of associating fluids using a saft-dft approach," Molecular Physics **99**, 1851–1865 (2001), https://doi.org/10.1080/00268970110075176.

[24] A. P. Willard and D. Chandler, "Instantaneous Liquid Interfaces," J. Phys. Chem. B **114**, 1954 (2010).

[25] A. Luzar and D. Chandler, "Effect of environment on hydrogen bond dynamics in liquid water," Phys. Rev. Lett. **76**, 928–931 (1996).

[26] A. Chandra, "Effects of Ion Atmosphere on Hydrogen-Bond Dynamics in Aqueous Electrolyte Solutions," Phys. Rev. Lett. **85**, 768–771 (2000).

[27] M. Tarek and D. J. Tobias, "Role of Protein-Water Hydrogen Bond Dynamics in the Protein Dynamical Transition," Phys. Rev. Lett. **88**, 138101 (2002).

[28] S. Pal, B. Bagchi, and S. Balasubramanian, "Hydration Layer of a Cationic Micelle, C_{10}TAB: Structure, Rigidity, Slow Reorientation, Hydrogen Bond Lifetime, and Solvation Dynamics," J. Phys. Chem. B **109**, 12879–12890 (2005).

[29] F. Sciortino and S. L. Fornili, "Hydrogen Bond Cooperativity in Simulated Water: Time Dependence Analysis of Pair Interactions," J. Chem. Phys. **90**, 2786–2792 (1989).

[30] A. K. Soper and M. G. Phillips, "A New Determination of the Structure of Water at 25 ° C," Chem. Phys **107**, 47–60 (1986).

[31] J. Teixeira, M. C. Bellisent-Funel, and S. H. Chen, "Dynamics of Water Studied by Neutron Scattering," J. Phys. Condens. Matter **2**, SA105 (1990).

[32] A. Luzar and D. Chandler, "Structure and hydrogen bond dynamics of water-dimethyl sulfoxide mixtures by computer simulations," J. Chem. Phys. **98**, 8160–8173 (1993).

[33] S. Balasubramanian, S. Pal, and B. Bagchi, "Hydrogen-Bond Dynamics Near a Micellar Surface: Origin of the Universal Slow Relaxation at Complex Aqueous Interfaces," Phys. Rev. Lett. **89**, 115505 (2002).

[34] D. Chandler, *Introduction to Morden Statistical Mechanics* (Oxford University press, Oxford, 1987).

[35] I. Benjamin, "Hydrogen Bond Dynamics at Water/Organic Liquid Interfaces," J. Phys. Chem. B **109**, 13711–13715 (2005).

[36] D. C. Rapaport, "Hydrogen Bonds in Water: Network Organization and Lifetimes," Mol. Phys. **50**, 1151–1162 (1983).

[37] A. Luzar, "Resolving the Hydrogen Bond Dynamics Conundrum," J. Chem. Phys. **113**, 10663 (2000).

[38] F. W. Starr, J. K. Nielsen, and H. E. Sta, "Hydrogen-Bond Dynamics for the Extended Simple Point-Charge Model of Water," Phys. Rev. E **62**, 579–587 (2000).

[39] D. Chandler, "Roles of Classical Dynamics and Quantum Dynamics on Activated Processes Occurring in Liquids," J. Stat. Phys. **42**, 49–67 (1986).

[40] D. Chandler, "Statistical Mechanics of Isomerization Dynamics in Liquids and the Transition State Approximation," J. Chem. Phys. **68**, 2959–2970 (1978).

[41] K. Laasonen, M. Sprik, M. Parrinello, and R. Car, ""ab initio" liquid water," J. Chem. Phys. **99**, 9080–9089 (1993), https://doi.org/10.1063/1.465574.

[42] D. Marx and J. Hutter, "Ab Initio Molecular Dynamics: Theory and Implemention," Modern Methods and Algorithms of Quantum Chemistry, J.Grotendorst (Ed.) John von Neumann Institute for Computing, Jülich, NIC Series **1**, 301–499 (2000).

[43] R. Khatib, E. H. G. Backus, M. Bonn, M. Perez-Haro, M.-P. Gaigeot, and M. Sulpizi, "Water Orientation and Hydrogen-Bond Structure at the Fluorite/Water Interface," Scientific Reports **6**, 24287 (2016).

[44] R. Khatib, T. Hasegawa, M. Sulpizi, E. H. G. Backus, M. Bonn, and Y. Nagata, "Molecular Dynamics Simulations of SFG Librational Modes Spectra of Water at the Water-Air Interface," J. Phys. Chem. C **120**, 18665–18673 (2016).

[45] R. Khatib and M. Sulpizi, "Sum Frequency Generation Spectra from Velocity-Velocity Correlation Functions," J. Phys. Chem. Lett. **8**, 1310–1314 (2017).

[46] S. Goedecker, M. Teter, and J. Hutter, "Separable dual-space gaussian pseudopotentials," Phys. Rev. B **54**, 1703–1710 (1996).

[47] C. Hartwigsen, S. Goedecker, and J. Hutter, "Relativistic separable dual-space gaussian pseudopotentials from H to Rn," Phys. Rev. B **58**, 3641–3662 (1998).

[48] M. Krack, "Pseudopotentials for H to Kr optimized for gradient-corrected exchange-correlation functionals," Theor. Chem. Acc. **114**, 145–152 (2005).

[49] A. D. Becke, "Density-functional exchange-energy approximation with correct asymptotic behavior," Phys. Rev. A **38**, 3098 (1988).

[50] C. Lee, W. Yang, and R. G. Parr, "Development of the colic-salvetti correlation-energy formula into a functional of the electron density," Phys. Rev. B **37**, 785 (1988).

[51] S. Grimme, J. Antony, S. Ehrlich, and H. Krieg, "A Consistent and Accurate Ab Initio Parametrization of Density Functional Dispersion Correction (DFT-D) for the 94 Elements H-Pu," J. Chem. Phys. **132**, 154104 (2010).

[52] J. Klimeš and A. Michaelides, "Perspective: Advances and Challenges in Treating van der Waals Dispersion Forces in Density Functional Theory," J. Chem. Phys. **137**, 120901–120912 (2012).

[53] J.-B. Lu, D. C. Cantu, M.-T. Nguyen, J. Li, V.-A. Glezakou, and R. Rousseau, "Norm-Conserving Pseudopotentials and Basis Sets To Explore Lanthanide Chemistry in Complex Environments," J. Chem. Theory Comput. **15**, 5987–5997 (2019).

[54] J. VandeVondele, M. Krack, F. Mohamed, M. Parrinello, T. Chassaing, and J. Hutter, "Quickstep: Fast and accurate density functional calculations using a mixed gaussian and plane waves approach," Comput. Phys. Commun. **167**, 103–128 (2005).

[55] T. D. Kühne, M. Iannuzzi, M. Del Ben, V. V. Rybkin, P. Seewald, F. Stein, T. Laino, R. Z. Khaliullin, O. Schütt, F. Schiffmann, D. Golze, J. Wilhelm, S. Chulkov, M. H. Bani-Hashemian, V. Weber, U. Borštnik, M. Taillefumier, A. S. Jakobovits, A. Lazzaro, H. Pabst, T. Müller, R. Schade, M. Guidon, S. Andermatt, N. Holmberg, G. K. Schenter, A. Hehn, A. Bussy, F. Belleflamme, G. Tabacchi, A. Glöß, M. Lass, I. Bethune, C. J. Mundy, C. Plessl, M. Watkins, J. VandeVondele, M. Krack, and J. Hutter, "Cp2k: An electronic structure and molecular dynamics software package - quickstep: Efficient and accurate electronic structure calculations," J. Chem. Phys. **152**, 194103 (2020), https://doi.org/10.1063/5.0007045.

[56] G. Lippert, J. Hutter, and M. Parrinello, "The gaussian and augmented-plane-wave density functional method for ab initio molecular dynamics simulations," Theor. Chem. Acc. **103**, 124 (1999).

[57] G. J. Martyna, M. L. Klein, and M. Tuckerman, "Nosé-hoover chains: The canonical ensemble via continuous dynamics," J. Chem. Phys. **97**, 2635 (1992).

[58] A. Serva, S. Pezzotti, S. Bougueroua, D. R. Galimberti, and M.-P. Gaigeot, "Combining ab-initio and classical molecular dynamics simulations to unravel the structure of the 2d-hb-network at the air-water interface," J. Molecular Structure **1165**, 71–78 (2018).

[59] A. Braslau, P. S. Pershan, G. Swislow, B. M. Ocko, and J. Als-Nielsen, "Capillary waves on the surface of simple liquids measured by x-ray reflectivity," Phys. Rev. A **38**, 2457–2470 (1988).